Linear State-Space Representation of the Axial Dynamics of Electrodynamic Thrust Bearings

Joachim Van Verdeghem, Corentin Dumont, Virginie Kluyskens, Bruno Dehez, *Member, IEEE*
Center for Research in Mechatronics (CEREM), Institute of Mechanics, Materials and Civil Engineering (IMMC), Université catholique de Louvain (UCL), Louvain-la-Neuve 1348, Belgium

Electrodynamic bearings can guide rotating objects without contact and without active control means. Consequently, their performance relies on passive phenomena that require specific models to be predicted. In the case of electrodynamic thrust bearings, early models involved assumptions on the rotor axial kinematics. This precludes their use for predicting the bearing behavior in dynamic conditions, which is critical when studying stability aspects. Other models require to solve numerically Faraday's current law and the rotor equation of motion to obtain the dynamics of the bearing, thereby excluding a fast identification of its stability properties. Recently, a parametric model without these kinematic assumptions was derived. It consists in a linear state-space representation that allows studying the dynamic performance of electrodynamic thrust bearings using conventional system analysis tools. However, this model links up the rotor displacement to the currents in a winding with only two phases. The present paper introduces a model free of this limitation, allowing to consider bearings with a higher number of phases, an improved copper usage, and potentially increased performance. Furthermore, the proposed model directly links up the rotor displacement to the force and torque exerted by the thrust bearing without requiring to solve for the currents. This also minimizes the number of state-space equations and model parameters. Finally, in addition to the modeling aspects, a set of bearing topologies that have not been explored yet and can be studied using the proposed model is introduced.

Index Terms—**Thrust, electrodynamic, passive, magnetic, bearings, modeling, linear, state-space.**

I. Introduction

Magnetic bearings offer numerous advantages such as the absence of mechanical wear and lubrication. Nowadays, the vast majority of the industrial implementations of such bearings are actively controlled. Active magnetic bearings (AMBs) achieve high stiffnesses and the active control of the rotor dynamics allows for higher speeds and power densities [1]. However, the control system associated with AMBs can be prohibitive in some applications where compactness, reliability and cost are critical [2]. An alternative solution consists in using high strength permanent magnets (PMs) to support the rotor [3] [4]. Despite their reasonable stiffness and their high energy efficiency, the use of PM bearings is limited by Earnshaw's theorem [5]. It states that an object cannot be fully levitating using only PMs or electromagnets fed with DC current. Consequently, at least one degree of freedom of the rotating object must be guided by a mechanical, active, electrodynamic or diamagnetic bearing e.g. [2]. Despite their low stiffness and stability issues, electrodynamic bearings (EDBs) maintain the advantages of the PM bearings as they can operate at room temperature, without contact and in a passive way. Radial EDBs have focused much research efforts [6]-[9]. In particular, stability aspects are critical for radial EDBs, which motivated the recent development of models especially suited for tackling this issue [10]-[13]. On the other hand, less attention was paid to thrust EDBs [14].

The interest in thrust EDBs dates back to 1971 [15]. Later, other bearings using the null-flux principle for higher energy efficiency were proposed [16]-[18]. In particular, much of the research interest focused on the topology proposed in [17] which was combined with PM radial bearings and a PM load reliever to levitate a rotor in a fully passive way [19]-[21]. Flywheels were cited as a potential application, and this configuration was successfully implemented and tested [19]. Along with this experiment came up models for studying the stiffness and stability properties of thrust EDBs. However, the scopes of these models are still narrowed by restrictive assumptions.

In a first model, the phase currents and the total force on the bearing rotor are obtained by neglecting the effects of the rotor axial speed on the induced forces [6]. However, assuming these quasi-static conditions precludes predicting the stability of a bearing operating in dynamic conditions. A second model requires a numerical integration of Faraday's current law and of the rotor equation of motion to calculate the Lorentz forces on the rotor [20]. Nevertheless, these integrations can be prohibitive when it comes to obtaining the stability properties of a thrust EDB in a wide range of rotor spin speed for instance. Furthermore, EDBs with a ferromagnetic yoke attached to the winding are not in the scope of this model as Lorentz force law does not apply in this case. A third modeling approach was proposed in [21]. It consists in a linear state-space representation of the system, allowing for straightforward stability analyzes. However, it is limited to windings with two phases, although considering a higher number of phases could improve the copper usage and the bearing performance.

In this context, this paper introduces a linear state-space representation of thrust EDBs without the previous limitations. It is obtained by applying an appropriate change of variables to the electromechanical equations governing the winding currents, the force, and the torque on the bearing rotor

Manuscript received February 5, 2014; revised May 2, 2014. Corresponding author: B. Dehez (email: bruno.dehez@uclouvain.be).

This article has been accepted for publication in a future issue of this journal, but has not been fully edited. Content may change prior to final publication. Citation information: DOI 10.1109/TMAG.2016.2582727, IEEE Transactions on Magnetics

[22]. These electromechanical equations are then coupled to the rotor motion equation. This yields a set of four linear state-space equations, allowing for straightforward stability analyzes. This state-space representation links up the rotor position to the force and torque exerted by the thrust bearing through seven parameters that do not depend on the rotor spin speed. On the basis of this set of parameters, the dynamic behavior of a thrust EDB is fully described and the performance of different bearings can be compared objectively.

The paper is structured as follows. Section II presents the bearing topologies. Following on from this, section III summarizes the hypotheses of the model. Section IV provides the analytical expression of the PM flux linked by the winding for each topology. The state-space model is then derived in sections V-VII and finally applied to a practical case in section VIII.

II. Bearing topologies

The model is derived for an heteropolar null-flux electrodynamic thrust bearing. It is constituted of two subassemblies rotating relative to each other, as shown in Fig. 1.

The first subassembly comprises two identical arrangements of PMs producing, each of them, an axial magnetic field having p pole pairs. The angular shift between the upper and lower magnet arrangements is denoted $\Delta\theta_{PM}$. These arrangements can be of different types, with surface-mounted, buried or inset permanent magnets, on the one hand, or respecting an Halbach array configuration, on the other hand. Permanent magnets could also be replaced by electromagnets supplied with DC currents. The PMs can also be external or internal as shown in Fig. 2a and b, respectively.

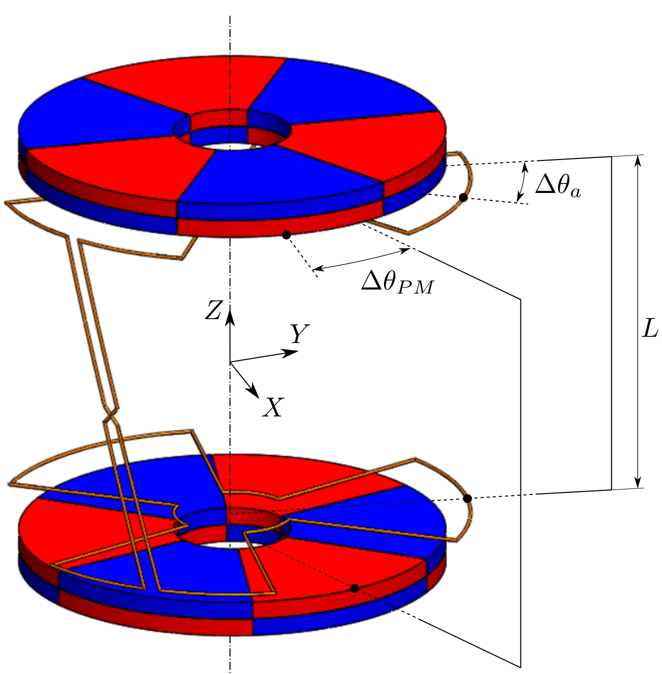

Fig. 1. Bearing topology with external PMs and series connection of a phase winding.

The second subassembly is made of two coils with p pole pairs, each predominantly magnetically linked to one PM arrangement, as represented in Fig. 1. The angular shift between the two coils is $\Delta\theta_a$. As represented in Fig. 1 and 2a, the two coils can be connected either in series or in opposition, forming a phase winding which is short-circuited. Such phase winding is duplicated N times so as to form a N-phase symmetrical armature winding. The phase windings are evenly distributed and the position of the k-th phase is given by:

$$\delta_k = \frac{2\pi(k-1)}{pN} + \delta_0, \tag{1}$$

where $k = \{1, \ldots, N\}$ and δ_0 is the first phase winding angular position. These windings may have various geometries but are identical. Moreover, they can be placed in air, as represented, but also behind a ferromagnetic yoke or in a slotted ferromagnetic circuit.

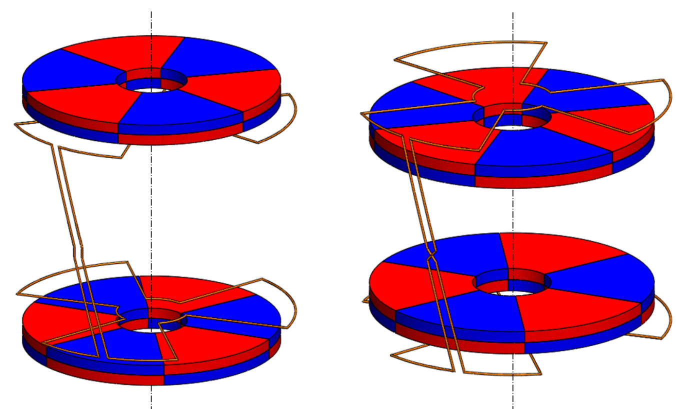

(a) (b)

Fig. 2. Bearing topology. (a) External PMs and opposition connection of a phase winding. (b) Internal PMs and series connection of a phase winding.

The distance L between both parts of the internal subassembly can also be reduced to zero. When the internal subassembly is the armature winding, it reduces to one single short-circuited coil. This is illustrated in Fig. 3a and yields the topology proposed in [20]. Conversely, when the internal subassembly includes the PM arrangements, they reduce to one as shown in Fig. 3b.

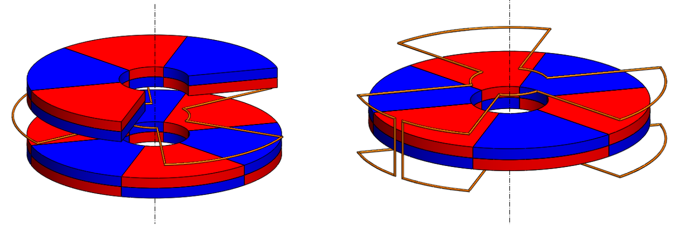

(a) (b)

Fig. 3. Bearing topology. (a) External PMs and a phase winding. (b) Opposition connection of a phase winding and a single internal PMs arrangement.

Finally, specific conditions on the angles $\Delta\theta_{PM}$ and $\Delta\theta_a$ have to be satisfied so as to ensure that the flux linked by

This article has been accepted for publication in a future issue of this journal, but has not been fully edited. Content may change prior to final publication. Citation information: DOI 10.1109/TMAG.2016.2582727, IEEE Transactions on Magnetics

the armature winding is null when it is centered along the Z axis with regard to the PM arrangements. In this way, there are no induced currents, and therefore no Joule losses in the windings as long as the rotating part is centered.

In the most general case, the internal subassembly includes two distinct parts, and each coil of the phase armature winding can be coupled with the two PM arrangements. Considering $k \in \mathbb{Z}$, the conditions on $\Delta\theta_{PM}$ and $\Delta\theta_a$ are:

$$\begin{aligned} \Delta\theta_{PM} &= \Delta\theta_a \\ \Delta\theta_a &= \frac{k\pi}{p} \end{aligned} \tag{2}$$

if the coils are connected in series, and:

$$\begin{aligned} \Delta\theta_{PM} &= \Delta\theta_a + \frac{\pi}{p} \\ \Delta\theta_a &= \frac{k\pi}{p} \end{aligned} \tag{3}$$

if the coils are connected in opposition. In presence of a magnetic insulation between the upper and lower parts of the bearing, each coil may be coupled to only one PM arrangement. In this case, the second identities in (2) and (3) do not hold anymore.

In the case of the merged topologies presented in Fig. 3, conditions (2) and (3) reduce to:

$$\Delta\theta_{PM} = \Delta\theta_a = 0 \tag{4}$$

if the armature windings constitute the internal subassembly. When the PMs constitute the internal subassembly:

$$\Delta\theta_a = \frac{(2k+1)\pi}{p} \tag{5}$$

if the coils are connected in series, and:

$$\Delta\theta_a = \frac{2k\pi}{p} \tag{6}$$

if the coils are connected in opposition.

III. Model assumptions

In order to establish the state-space model of the EDB, the following assumptions are made:

1) only axial and radial displacements are considered, i.e. the spin axes of the stator and rotor remain parallel;
2) the axial and radial displacements are supposed to be small;
3) the materials have linear magnetic properties i.e. magnetic hysteresis and saturation are neglected;
4) the inductance variations due to rotor axial and radial displacements are neglected;
5) the inductance variations due to the rotor angular position around its spin axis are neglected;
6) the proximity and skin effects in the conductors are neglected;
7) the eddy currents are neglected;
8) only the fundamental component of the PMs arrangements magnetic field is considered;
9) the spin speed of the rotor ω is an input of the system and varies slowly compared to the axial dynamics.

The assumptions made on the inductances are verified in the absence of ferromagnetic pieces. However, the assumption 4 becomes weaker if there is a ferromagnetic circuit linked to the PMs arrangements. This is even the more true when ferromagnetic yokes are also present at the armature and even more important if the windings are placed in slotted ferromagnetic circuits. By contrast, the assumption 5 becomes weaker only when there is a ferromagnetic circuit with saliencies linked to the PMs arrangements.

IV. PM flux linkage

A. PM magnetic flux density

The purpose of this subsection is to derive the expression of the magnetic flux density in the frame of the armature windings, whether they are at the rotor or at the stator. As stated in section II, the thrust bearing being analyzed is constituted of two subassemblies: the PMs and the armature winding. Each is assigned a frame whose (i) vertical axis Z is aligned with the symmetry axis, (ii) origin is located at half-height of both parts constituting the subassembly and (iii) X axis is aligned with the magnetic axis. More precisely, the coordinates related to the PMs arrangements and armature are $\{r, \theta, Z\}$ and $\{\xi, \psi, a\}$ respectively. As shown in Fig. 4, the position of the rotor in the stator frame is (ϵ, ϕ, z). According to assumption 9, the rotor spin angle around its vertical axis is $\alpha = \omega t + \alpha_0$, with α_0 the initial position and ω the spin speed.

For the sake of clarity, let us consider, to derive the following equations, the particular topology with the armature winding as internal subassembly, an angular shift $\Delta\theta_{PM} = 0$ between both PMs arrangements and a series connection. However, the same analysis can be applied to the other topologies yielding an identical result. As indicated in (2), the angular shift $\Delta\theta_a = 0$. Furthermore, according to assumption 8, the axial component of the magnetic flux density due to the PMs arrangements is modeled as:

$$B(r, \theta, Z) = \cos(p\theta) f(Z) g(r), \tag{7}$$

where p is the number of pole pairs and $f(Z)$ as well as $g(r)$ depend on the PMs arrangements and on the presence of ferromagnetic parts at the armature. Besides, the function $f(Z)$ is odd as $\Delta\theta_{PM} = 0$.

1) PMs attached to the stator

Let us now study the case with the PMs attached to the stator. The coordinate transformation from the fixed frame to the rotating frame is:

$$\begin{aligned} r &= \sqrt{\epsilon^2 + \xi^2 + 2\xi\epsilon\cos(\psi + \alpha - \phi)} \\ \theta &= \tan^{-1}\left(\frac{\epsilon\sin(\phi) + \xi\sin(\psi + \alpha)}{\epsilon\cos(\phi) + \xi\cos(\psi + \alpha)}\right) \\ Z &= z + a \end{aligned} \tag{8}$$

This article has been accepted for publication in a future issue of this journal, but has not been fully edited. Content may change prior to final publication. Citation information: DOI 10.1109/TMAG.2016.2582727, IEEE Transactions on Magnetics

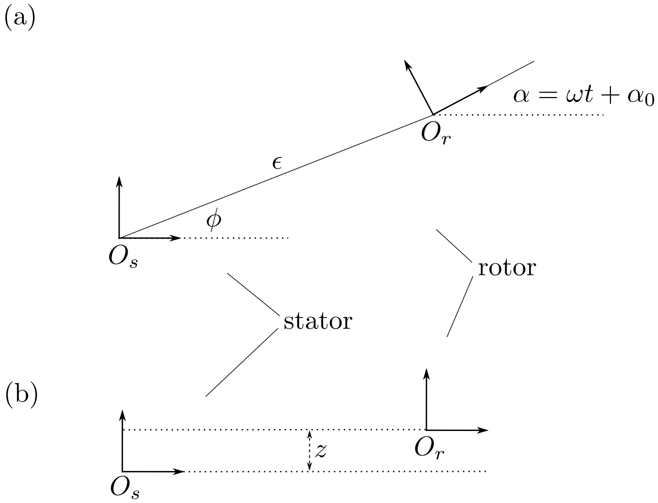

Fig. 4. Stator and rotor frames. (a) Upside view. (b) Lateral view.

Substituting (8) into (7) allows determining the magnetic flux density due to the PMs in the rotor frame:

$$\begin{aligned} B(\xi,\psi,a) \;=\; & \cos\left(p\tan^{-1}\left(\frac{\epsilon\sin(\phi)+\xi\sin(\psi+\alpha)}{\epsilon\cos(\phi)+\xi\cos(\psi+\alpha)}\right)\right) \\ & \times\; g\left(\sqrt{\epsilon^2+\xi^2+2\xi\epsilon\cos(\psi+\alpha-\phi)}\right) \\ & \times\; f(z+a). \end{aligned} \tag{9}$$

According to assumption 2, the axial and radial displacements are small. Therefore, the first order Taylor expansion of (9) around the nominal position of the EDB $(\epsilon, z) = (0, 0)$ can be derived and leads to:

$$\begin{aligned} B(\xi,\psi,a) \approx\; & \cos(p(\psi+\alpha))g(\xi)f(a) \\ & + z\cos(p(\psi+\alpha))g(\xi)\frac{\partial f}{\partial Z}(a) \\ & + \epsilon\cos((\psi+\alpha)(p+1)-\phi)\frac{f(a)}{2}\left(\frac{\partial g}{\partial r}(\xi)-p\frac{g(\xi)}{\xi}\right) \\ & + \epsilon\cos((\psi+\alpha)(p-1)+\phi)\frac{f(a)}{2}\left(\frac{\partial g}{\partial r}(\xi)+p\frac{g(\xi)}{\xi}\right). \end{aligned} \tag{10}$$

2) PMs attached to the rotor

Let us then study the case with the PMs attached to the rotor. The coordinate transformation from the rotating frame to the fixed frame is:

$$\begin{aligned} r &= \sqrt{\xi^2+\epsilon^2-2\epsilon\xi\cos(\psi-\phi)} \\ \theta &= \tan^{-1}\left(\frac{\xi\sin(\psi-\alpha)-\epsilon\sin(\phi-\alpha)}{\xi\cos(\psi-\alpha)-\epsilon\cos(\phi-\alpha)}\right) \\ Z &= a-z \end{aligned} \tag{11}$$

Substituting (11) into (7) yields the magnetic flux density in the stator frame:

$$\begin{aligned} B(\xi,\psi,a) \;=\; & \cos\left(p\tan^{-1}\left(\frac{\xi\sin(\psi-\alpha)-\epsilon\sin(\phi-\alpha)}{\xi\cos(\psi-\alpha)-\epsilon\cos(\phi-\alpha)}\right)\right) \\ & \times\; g\left(\sqrt{\xi^2+\epsilon^2-2\epsilon\xi\cos(\psi-\phi)}\right) \\ & \times\; f(a-z). \end{aligned} \tag{12}$$

Deriving the first order Taylor expansion of (12) around the nominal position of the EDB $(\epsilon, z) = (0, 0)$ leads to:

$$\begin{aligned} B(\xi,\psi,a) \approx\; & \cos(p(\psi-\alpha))g(\xi)f(a) \\ & + z\cos(p(\psi-\alpha))g(\xi)\frac{\partial f}{\partial Z}(a) \\ & + \epsilon\cos(\psi(p+1)-p\alpha-\phi)\frac{f(a)}{2}\left(-\frac{\partial g}{\partial r}(\xi)-p\frac{g(\xi)}{\xi}\right) \\ & + \epsilon\cos(\psi(p-1)-p\alpha+\phi)\frac{f(a)}{2}\left(-\frac{\partial g}{\partial r}(\xi)+p\frac{g(\xi)}{\xi}\right). \end{aligned} \tag{13}$$

B. General form of PM flux linkage

Let us consider that the coils are made of loops whose surface is given by:

$$S \equiv \begin{cases} R_i \le \xi \le R_o \\ -t(\xi) \le \psi \le t(\xi) \end{cases}, \tag{14}$$

where $t(\xi)$ is the function describing the shape of the loop. This single loop can be replicated N_l times at the same location. The set constituted of those N_l loops is duplicated p times at positions β_j such that they are evenly distributed around the symmetry axis:

$$\beta_j = \frac{2\pi(j-1)}{p}, \tag{15}$$

with $j = \{1, \dots, p\}$. Such an arrangement is placed at $a = L/2$ and constitutes a first coil. Remembering that $\Delta\theta_a = 0$, the same arrangement is also placed at $a = -L/2$, forming a second coil. Both coils are connected in series constituting one phase winding and are reproduced N times at positions δ_k, as explained in section II, in order to form the armature.

The PM flux linked by a single loop defined by its surface S can be obtained as follows:

$$\Phi = \iint_S \mathbf{B}\cdot\mathbf{n}\,dS, \tag{16}$$

where $\mathbf{n}$ is the normal vector to the integration surface. As this vector is aligned with the axial component of the magnetic field, the PM flux linkage $\Phi_{w,k}$ of the k-th coil located at a position a is given by:

$$\Phi_{w,k}(a) = N_l\sum_{j=1}^{p}\int_{R_i}^{R_o}\int_{-t(\xi)+\delta_k+\beta_j}^{t(\xi)+\delta_k+\beta_j} B(\xi,\psi,a)d\psi\xi d\xi \tag{17}$$

Knowing that the coils of one phase are connected in series, the total flux Φ_k linked by the k-th phase winding is computed as the sum of the flux intercepted by the k-th coils located at $a = L/2$ and $a = -L/2$:

$$\Phi_k = \Phi_{w,k}(L/2) + \Phi_{w,k}(-L/2). \tag{18}$$

This article has been accepted for publication in a future issue of this journal, but has not been fully edited. Content may change prior to final publication. Citation information: DOI 10.1109/TMAG.2016.2582727, IEEE Transactions on Magnetics

1) PMs attached to the stator

Using (10) for the case with the PMs attached to the stator, the flux linkage (17) becomes:

$$\begin{aligned}\Phi_{w,k}(a) \;=\; N_l \sum_{j=1}^{p} & \left[\cos(p(\alpha+\delta_k+\beta_j)) f(a) K_{s1}\right. \\ & +z\cos(p(\alpha+\delta_k+\beta_j))\frac{\partial f}{\partial Z}(a)K_{s2} \\ & +\epsilon\cos((p+1)(\alpha+\delta_k+\beta_j)-\phi)f(a)K_{s3} \\ & \left.+\epsilon\cos((p-1)(\alpha+\delta_k+\beta_j)+\phi)f(a)K_{s4}\right],\end{aligned} \tag{19}$$

where K_{si} are constants resulting from the integrations. The function $f(Z)$ is odd and thus its first derivative is even, yielding:

$$\begin{aligned} & f(L/2)+f(-L/2)=0 \\ & \frac{\partial f}{\partial Z}(L/2)+\frac{\partial f}{\partial Z}(-L/2)=2\cdot\frac{\partial f}{\partial Z}(L/2).\end{aligned} \tag{20}$$

Consequently, the only remaining terms in the total flux (18) linked by the k-th phase winding are those proportional to z. Due to the properties of the cosine, it reduces to:

$$\Phi_k = zK_\phi\cos(p(\alpha+\delta_k)), \tag{21}$$

where K_ϕ is a constant which depends on the geometric and magnetic parameters of the EDB. Using identical arguments, it is straightforward to proof that the second order Taylor expansion of the magnetic flux density yields the same result. Indeed, the term in ϵ^2 is proportional to $f(a)$ and is then canceled. The term in z^2 is proportional to $\partial^2 f/\partial Z^2(a)$ and the second derivative of an odd function is odd: this term is thus also canceled. Finally, the term in ϵz is proportional to $\partial f/\partial Z(a)$ but the sum over j removes it due to the fact that $\sum_{j=1}^{p}\cos(x+(p\pm1)2\pi(j-1)/p)=0$. Therefore, connecting all the loops of one phase in series allows removing the effect of the eccentricity ϵ at second order.

2) PMs attached to the rotor

Let us follow the same method for the case where the PMs are attached to the rotor. Substituting (13) into (17) yields:

$$\begin{aligned}\Phi_{w,k}(a) \;=\; N_l \sum_{j=1}^{p} & \left[\cos(p(\delta_k+\beta_j-\alpha)) f(a) K_{r1}\right. \\ & +z\cos(p(\delta_k+\beta_j-\alpha))\frac{\partial f}{\partial Z}(a)K_{r2} \\ & +\epsilon\cos((p+1)(\delta_k+\beta_j)-p\alpha-\phi)f(a)K_{r3} \\ & \left.+\,\epsilon\cos((p-1)(\delta_k+\beta_j)-p\alpha+\phi)f(a)K_{r4}\right],\end{aligned} \tag{22}$$

where K_{ri} are constants resulting from the integrations. Based on (20), (22) and the properties of the cosine, the total flux linkage (18) reduces to:

$$\Phi_k = zK_\phi\cos(p(\delta_k-\alpha)), \tag{23}$$

where K_ϕ is a constant which depends on the geometric and magnetic parameters of the EDB. As for the case with the PMs attached to the stator, it is straightforward to proof that the second order Taylor expansion of the magnetic field yields an identical result.

3) Analysis

The expressions (21) and (23) of the flux linkage for both cases only differ through the sign of the rotor angular position α and therefore its direction of rotation. Hence, later in this paper, both cases are reduced to the same general case described by (23). This expression only depends on the rotor axial displacement and angular position and not on the eccentricity. Moreover, as expected, the flux linkage is null when there is no axial displacement to respect the null-flux principle.

V. Governing equations

In this section, the electrical and electromechanical equations describing the dynamics of the EDB are derived.

A. Electrical equations

As stated in section II, each of the N phase windings are short-circuited. Applying Faraday's law to the k-th phase yields:

$$u_k = 0 = R_k I_k + \frac{d\Psi_k}{dt}, \tag{24}$$

where R_k is the phase resistance and Ψ_k the total magnetic flux linkage. This flux can be separated into two contributions, one due to the PMs and the other due to the inductances:

$$0 = R_k I_k + \frac{d\left(\sum_{l=1}^{N} L_{kl} I_l\right)}{dt} + \frac{d\Phi_k}{dt}, \tag{25}$$

where L_{kl} are the phase self and mutual inductances and Φ_k is the magnetic flux linkage due to PMs. According to assumptions 4 and 5, the inductances do not depend on the rotor position and are therefore time-independent, leading to:

$$0 = R_k I_k + \sum_{l=1}^{N} L_{kl}\frac{dI_l}{dt} + \frac{d\Phi_k}{dt}. \tag{26}$$

This equation can be expressed in matrix form as:

$$\mathbf{0} = \mathbf{R}\mathbf{I} + \mathbf{L}\frac{d\mathbf{I}}{dt} + \frac{d\mathbf{\Phi}}{dt}. \tag{27}$$

As previously specified, the winding phases are identical and so are the phase resistance:

$$\mathbf{R} = R\mathbb{1}, \tag{28}$$

where $\mathbb{1}$ is the identity matrix. Besides, the phases are evenly distributed and their properties constant. Hence, the matrix $\mathbf{L}$ is symmetric and circulant:

$$\begin{aligned} L_{kl} &= L_{lk} \\ L_{kl} &= L_{k+i,l+i} \\ L_{1l} &= L_{1,N+2-l},\end{aligned} \tag{29}$$

where $i,k,l \in \{1,\ldots,N\}$. Finally, without modifying the properties (29), external inductors of equal impedances can be connected in series with each phase winding. This enables to change the dynamic properties of the EDB [9].

This article has been accepted for publication in a future issue of this journal, but has not been fully edited. Content may change prior to final publication. Citation information: DOI 10.1109/TMAG.2016.2582727, IEEE Transactions on Magnetics

B. Electromechanical equations

As shown in section IV, the flux linkage $\mathbf{\Phi}$ due to the PMs only depends on the rotor axial displacement z and angular position α. Therefore, the electrodynamic forces and torques are reduced to the axial ones:

$$F = \sum_{k=1}^{N} \frac{\partial \Phi_k}{\partial z} I_k \tag{30}$$

$$T = \sum_{k=1}^{N} \frac{\partial \Phi_k}{\partial \alpha} I_k, \tag{31}$$

Considering Φ_k and I_k as complex variables, these expressions can be rewritten in the following matrix form:

$$F = \left[\frac{\partial \mathbf{\Phi}}{\partial z}\right]^T \mathbf{I}^* \tag{32}$$

$$T = \left[\frac{\partial \mathbf{\Phi}}{\partial \alpha}\right]^T \mathbf{I}^*, \tag{33}$$

where $\mathbf{I}^*$ represents the complex conjugate of $\mathbf{I}$.

According to assumptions 4 and 5, the inductance matrix $\mathbf{L}$ is constant. Therefore, the reluctant efforts are equal to zero. Besides, detent efforts could appear due to interaction of the PMs arrangements with ferromagnetic parts located at the armature. Hereinafter, their contributions to the electromagnetic efforts are taken into account in the form of external efforts on the rotor, see section VII-B.

VI. Variables elimination

The study of the present EDB has some similarities with the study of N-phase rotating field machines. As for the rotating field machines, it is possible to reduce the number of variables needed to describe the operation of EDBs through an appropriate transformation. This is done in this section, following the approach described in [22]. Let us define the variables transformation:

$$\begin{aligned} \mathbf{I} &= \mathbf{U}\mathbf{I}^{\mathbf{s}} \\ \mathbf{\Phi} &= \mathbf{U}\mathbf{\Phi}^{\mathbf{s}}, \end{aligned} \tag{34}$$

with:

$$U_{kl} = \frac{1}{\sqrt{N}} e^{-j(k-1)(l-1)\frac{2\pi}{N}}, \tag{35}$$

where $j = \sqrt{-1}$ and $k, l \in \{1, \ldots, N\}$.

A. Electrical equations

Substituting (34) into (27) yields:

$$\mathbf{0} = R\mathbf{U}\mathbf{I}^{\mathbf{s}} + \mathbf{L}\mathbf{U}\frac{d\mathbf{I}^{\mathbf{s}}}{dt} + \mathbf{U}\frac{d\mathbf{\Phi}^{\mathbf{s}}}{dt}. \tag{36}$$

The inverse of matrix $\mathbf{U}$ is given in [22]:

$$U_{kl}^{-1} = \frac{1}{\sqrt{N}} e^{j(k-1)(l-1)\frac{2\pi}{N}} = U_{kl}^*. \tag{37}$$

Pre-multiplying (36) by $\mathbf{U^{-1}}$ leads to:

$$\mathbf{0} = R\mathbf{I}^{\mathbf{s}} + \mathbf{U^{-1}}\mathbf{L}\mathbf{U}\frac{d\mathbf{I}^{\mathbf{s}}}{dt} + \frac{d\mathbf{\Phi}^{\mathbf{s}}}{dt}. \tag{38}$$

Defining $\mathbf{L}^{\mathbf{s}} = \mathbf{U^{-1}}\mathbf{L}\mathbf{U}$, (38) becomes:

$$\mathbf{0} = R\mathbf{I}^{\mathbf{s}} + \mathbf{L}^{\mathbf{s}}\frac{d\mathbf{I}^{\mathbf{s}}}{dt} + \frac{d\mathbf{\Phi}^{\mathbf{s}}}{dt}, \tag{39}$$

where the N equations are decoupled due to the properties of $\mathbf{U}$ and (29). The diagonal terms of $\mathbf{L}^{\mathbf{s}}$ can be calculated as:

$$L_{ii}^s = \sum_{k=1}^{N} L_{1k} e^{-j(i-1)(k-1)\frac{2\pi}{N}}, \tag{40}$$

where $k = 1, \ldots, N$. The flux linkage $\mathbf{\Phi}^{\mathbf{s}}$ can be derived relying on (23) and (34). The details are available in the appendix and yield:

$$\mathbf{\Phi}^{\mathbf{s}} = z\frac{K_\Phi\sqrt{N}}{2}\begin{bmatrix} 0 \\ \exp(jp(\alpha-\delta_0)) \\ 0 \\ \vdots \\ 0 \\ \exp(-jp(\alpha-\delta_0)) \end{bmatrix}. \tag{41}$$

Therefore, among the N decoupled equations in (39), two present a non-homogeneous term. As a result, only the two corresponding currents I_2^s and I_N^s are non-zero. Defining:

$$\mathbf{\Phi}^{\mathbf{r}} = \begin{bmatrix} \Phi_2^s \\ \Phi_N^s \end{bmatrix} = z\frac{K_\Phi\sqrt{N}}{2}\begin{bmatrix} \exp(jp(\alpha-\delta_0)) \\ \exp(-jp(\alpha-\delta_0)) \end{bmatrix} \tag{42}$$

$$\mathbf{I}^{\mathbf{r}} = \begin{bmatrix} I_2^s \\ I_N^s \end{bmatrix}, \tag{43}$$

the number electrical of equations is reduced from N to 2 which gives:

$$\mathbf{0} = R\mathbf{I}^{\mathbf{r}} + \mathbf{L}^{\mathbf{r}}\frac{d\mathbf{I}^{\mathbf{r}}}{dt} + \frac{d\mathbf{\Phi}^{\mathbf{r}}}{dt}. \tag{44}$$

The inductance of both phases are equal:

$$L_c = L_{22}^r = L_{NN}^r = \sum_{k=1}^{N} L_{1k}\cos\left((k-1)\frac{2\pi}{N}\right), \tag{45}$$

where L_c is the cyclic inductance of the winding. The two elements of the flux linkage (42) are complex conjugates. Therefore, both equations in (44) are complex conjugates and so are the two resulting currents. The system (44) reduces to:

$$\begin{cases} 0 = RI_1^r + L_c\dfrac{dI_1^r}{dt} + \dfrac{d\Phi_1^r}{dt} \\ I_1^r = I_2^{r*} \end{cases}. \tag{46}$$

Substituting the flux linkage Φ_1^r by its expression (42) into (46) and multiplying by $\exp(-jp(\alpha-\delta_0))$ yields:

$$\begin{aligned} 0 = R[I_1^r\exp(-jp(\alpha-\delta_0))] + L_c\Bigg[\frac{d}{dt}[I_1^r\exp(-jp(\alpha-\delta_0))] \\ + jp\dot{\alpha}[I_1^r\exp(-jp(\alpha-\delta_0))]\Bigg] + \frac{K_\Phi\sqrt{N}}{2}(\dot{z} + jp\dot{\alpha}z). \end{aligned} \tag{47}$$

Let us define:

$$Y = I_1^r\exp(-jp(\alpha-\delta_0)). \tag{48}$$

This article has been accepted for publication in a future issue of this journal, but has not been fully edited. Content may change prior to final publication. Citation information: DOI 10.1109/TMAG.2016.2582727, IEEE Transactions on Magnetics

Substituting (48) into (47), this equation can be separated into real and imaginary parts as follows:

$$\begin{cases} 0 = R\cdot\Re(Y) + L_c\left[\dfrac{d\Re(Y)}{dt} - \dot{\alpha}p\Im(Y)\right] + \dfrac{K_\Phi\sqrt{N}}{2}\dot{z} \\ 0 = R\cdot\Im(Y) + L_c\left[\dfrac{d\Im(Y)}{dt} + \dot{\alpha}p\Re(Y)\right] + \dfrac{K_\Phi\sqrt{N}}{2}\dot{\alpha}pz \end{cases}. \tag{49}$$

B. Electromechanical equations

1) Force

The force can be calculated by substituting (34) into (32):

$$\begin{aligned} F &= \left[\frac{\partial(\mathbf{U}\mathbf{\Phi^s})}{\partial z}\right]^T(\mathbf{U}\mathbf{I^s})^* \\ &= \frac{\partial[\mathbf{\Phi^s}]^T}{\partial z}\mathbf{U}^T\mathbf{U}^*\mathbf{I^{s*}} \end{aligned} \tag{50}$$

Knowing that $\mathbf{U}^T = \mathbf{U}$ and $\mathbf{U}^* = \mathbf{U}^{-1}$, (50) becomes:

$$F = \frac{\partial[\mathbf{\Phi^s}]^T}{\partial z}\mathbf{I^{s*}} \tag{51}$$

As stated in (41), $\mathbf{\Phi^s}$ has only two non-zero components which yields:

$$F = \frac{\partial[\mathbf{\Phi^r}]^T}{\partial z}\mathbf{I^{r*}} \tag{52}$$

The flux linkage can be replaced by its expression (42). Moreover, remembering that $I_2^{r*} = I_1^r$, (52) becomes:

$$F = \frac{K_\Phi\sqrt{N}}{2}[I_1^{r*}\exp(jp(\alpha-\delta_0)) + I_1^r\exp(-jp(\alpha-\delta_0))]. \tag{53}$$

Substituting (48) into (53) yields:

$$\begin{aligned} F &= \frac{K_\Phi\sqrt{N}}{2}[Y^* + Y] \\ &= K_\Phi\sqrt{N}\cdot\Re(Y). \end{aligned} \tag{54}$$

2) Torque

The same development applied to the expression of the torque (33) gives:

$$T = \frac{\partial[\mathbf{\Phi^r}]^T}{\partial \alpha}\mathbf{I^{r*}} \tag{55}$$

Replacing the flux linkage by its expression (42) and taking into account that $I_2^{r*} = I_1^r$ leads to:

$$\begin{aligned} T &= jpz\frac{K_\Phi\sqrt{N}}{2}[I_1^{r*}\exp(jp(\alpha-\delta_0)) - I_1^r\exp(jp(\delta_0-\alpha))] \\ &= jpz\frac{K_\Phi\sqrt{N}}{2}[Y^* - Y] \\ &= pzK_\Phi\sqrt{N}\cdot\Im(Y) \end{aligned} \tag{56}$$

VII. State-space model derivation

Isolating $\Re(Y)$ in (54) and $\Im(Y)$ in (56) yields:

$$\Re(Y) = F\cdot\frac{1}{K_\Phi\sqrt{N}}. \tag{57}$$

$$\Im(Y) = \frac{T}{z}\cdot\frac{1}{pK_\Phi\sqrt{N}} \tag{58}$$

Substituting those expressions into (49) and multiplying by $K_\Phi\sqrt{N}$ gives:

$$\begin{cases} 0 = RF + L_c\left[\dot{F} - \dot{\alpha}\left(\dfrac{T}{z}\right)\right] + \dfrac{K_\Phi^2 N}{2}\dot{z} \\ 0 = \dfrac{R}{p}\left(\dfrac{T}{z}\right) + L_c\left[\dfrac{1}{p}\dot{\left(\dfrac{T}{z}\right)} + \dot{\alpha}pF\right] + \dfrac{K_\Phi^2 N}{2}\dot{\alpha}pz \end{cases}. \tag{59}$$

The system of ordinary differential equations in (59) can be rearranged as follows:

$$\begin{cases} \dot{F} = -\dfrac{R}{L_c}F + \dot{\alpha}\left(\dfrac{T}{z}\right) - \dfrac{K_\Phi^2 N}{2L_c}\dot{z} \\ \dot{\left(\dfrac{T}{z}\right)} = -\dfrac{R}{L_c}\left(\dfrac{T}{z}\right) - \dot{\alpha}p^2F - \dfrac{K_\Phi^2 N}{2L_c}\dot{\alpha}p^2 z \end{cases}. \tag{60}$$

This last system of two equations describes the complete dynamics of the EDB by linking the axial displacement, the force, the torque (position-related) and their derivatives. Based on assumption 9, the rotor angular speed $\dot{\alpha}$ is replaced by ω. Therefore, (60) is a linear system with constant coefficients.

A. Rotor mechanical model coupling

The system in (60) only describes the dynamics of the EDB and must then be coupled with a mechanical model of the rotor. The dynamics of an one degree of freedom damped rotor is governed by:

$$M\ddot{z} + C\dot{z} = F + F_e, \tag{61}$$

where M is the rotor mass, C the damping factor and F_e are the external axial forces acting on the rotor. Coupling (61) with (60) leads to:

$$\begin{bmatrix} \dot{F} \\ \dot{\left(\dfrac{T}{z}\right)} \\ \dot{z} \\ \ddot{z} \end{bmatrix} = \mathbf{A}\begin{bmatrix} F \\ \left(\dfrac{T}{z}\right) \\ z \\ \dot{z} \end{bmatrix} + \mathbf{B}\cdot F_e, \tag{62}$$

where:

$$\mathbf{A} = \begin{bmatrix} -\dfrac{R}{L_c} & \omega & 0 & -\dfrac{K_\Phi^2 N}{2L_c} \\ -\omega p^2 & -\dfrac{R}{L_c} & -\omega p^2\dfrac{K_\Phi^2 N}{2L_c} & 0 \\ 0 & 0 & 0 & 1 \\ \dfrac{1}{M} & 0 & 0 & -\dfrac{C}{M} \end{bmatrix}, \tag{63}$$

$$\mathbf{B} = \frac{1}{M}\begin{bmatrix}0 & 0 & 0 & 1\end{bmatrix}^T. \tag{64}$$

B. Detent force and torque

As stated in section V-B, detent efforts could appear due to the interaction of the PMs arrangements with ferromagnetic parts located at the armature. Under the small displacement assumption, the detent force can be associated with a constant negative stiffness K_d. Up to this point, it was taken into account in the external forces F_e, which can therefore be separated as follows:

$$F_e = F_e^{'} - K_d z, \tag{65}$$

where $F_e^{'}$ are the external axial forces without the contribution of the detent force. Therefore, the electromagnetic force $F^{'}$ is:

$$F^{'} = F - K_d z \tag{66}$$

Substituting (65) and (66) into (62), the state-space model of the EDB becomes:

$$\begin{bmatrix} \dot{F}^{'} \\ \dot{\left(\frac{T}{z}\right)} \\ \dot{z} \\ \ddot{z} \end{bmatrix} = \mathbf{A}^{'} \begin{bmatrix} F^{'} \\ \left(\frac{T}{z}\right) \\ z \\ \dot{z} \end{bmatrix} + \mathbf{B} \cdot F_e^{'}, \tag{67}$$

where:

$$\mathbf{A}^{'} = \mathbf{A} + K_d \begin{bmatrix} 0 & 0 & -R/L_c & -1 \\ 0 & 0 & -\omega p^2 & 0 \\ 0 & 0 & 0 & 0 \\ 0 & 0 & 0 & 0 \end{bmatrix}. \tag{68}$$

By contrast, the effect of a possible detent torque, which would come from the presence of saliencies located at the armature, can not be taken into account in this model as the spin speed is considered to be constant, according to assumption 9.

C. Model parameters determination

The model (67) comprises eight parameters. Among these, two are the rotor mass M and the damping C, whose determination is not detailed in this paper. The six remaining parameters only depend on the geometry as well as the magnetic and electrical properties of the thrust bearing: the number p of pole pairs, the number N of winding phases, the phase resistance R, the cyclic inductance L_c, the coefficient K_Φ and the detent stiffness K_d.

These parameters can be determined in two different ways. On the one hand, they can be calculated through analytical formulas and models. On the other hand, they can be identified using either experimental data or finite element methods, as explained hereinafter.

Through the expression (45), the cyclic inductance is directly linked to the self inductance L_{11} and the mutual inductances L_{1k}. The self inductance can be calculated by injecting a current I in one phase and evaluating the magnetic energy $W_{m,1}$ stored in the system:

$$L_{11} = \frac{2W_{m,1}}{I^2}. \tag{69}$$

The mutual inductances can be determined by injecting a current I in both phases 1 and k and evaluating the magnetic energy $W_{m,2}$ stored in the system:

$$L_{1k} = \frac{W_{m,2}}{I^2} - L_{11}. \tag{70}$$

In both case, the remanent magnetization of the permanent magnets has to be canceled.

The detent stiffness K_d corresponds to the stiffness of the EDB in quasi-static conditions at zero spin speed, i.e. $\dot{z} = 0$ and $\omega = 0$. Therefore, based on (66) and considering an axial displacement z, the coefficient K_d is given by:

$$K_d = -\frac{F'(z)}{z}. \tag{71}$$

The coefficient K_Φ can be identified through the relation (23) by evaluating, for an axial displacement z, the flux linked by a phase winding in an angular position maximizing this flux linkage and in quasi-static conditions, i.e. $\dot{z} = 0$:

$$K_\Phi = \frac{\Phi(z)}{z}. \tag{72}$$

D. Phase currents derivation

The state-space representation (67) describes the axial dynamics of the EDB without solving for the phase currents. However, calculating the currents may be required to perform a thermal analysis e.g. Knowing the force F and the torque T, they can be derived as follows. Considering (57) and (58) leads to:

$$Y = \frac{F}{K_\Phi \sqrt{N}} + j \frac{T}{pzK_\Phi \sqrt{N}}. \tag{73}$$

Considering (48), the second identity in (46), and (43) yields:

$$\begin{aligned} I_2^s &= I_1^r = Y \exp\left(jp(\alpha - \delta_0)\right) \\ I_N^s &= I_2^r = I_2^{s*} \end{aligned} \tag{74}$$

Through (34), the instantaneous current in the k-th phase is finally obtained:

$$I_k = \frac{2}{K_\Phi N} \left(F \cos\left(p(\alpha - \delta_k)\right) - \frac{T}{pz} \sin\left(p(\alpha - \delta_k)\right) \right). \tag{75}$$

VIII. Practical case

Let us consider the EDB shown in Fig. 5. It corresponds to the topology with the armature windings as internal subassembly and the distance L reduced to zero. The external subassembly includes PMs arrangements and ferromagnetic yokes that are attached to the stator. The PMs remanent magnetization is 1.42 [T] and the number p of pole pairs is 3. The armature winding is composed of ten phases ($N = 10$) whose geometry is shown in Fig. 6. Each phase is constituted of only one loop ($N_l = 1$). The forward and return conductors of the phase windings are shifted vertically by a distance h_t, which allows interlocking the phases and therefore increasing their number. The dimensions of the EDB are given in Table I.

Table I
Bearing dimensions [mm].

R_{wire}	R_i	R_{ii}	R_{ee}	R_e	h_y	h_{PM}	h_t	e
0.25	5	10	40	50	3	6	1	10

This article has been accepted for publication in a future issue of this journal, but has not been fully edited. Content may change prior to final publication. Citation information: DOI 10.1109/TMAG.2016.2582727, IEEE Transactions on Magnetics

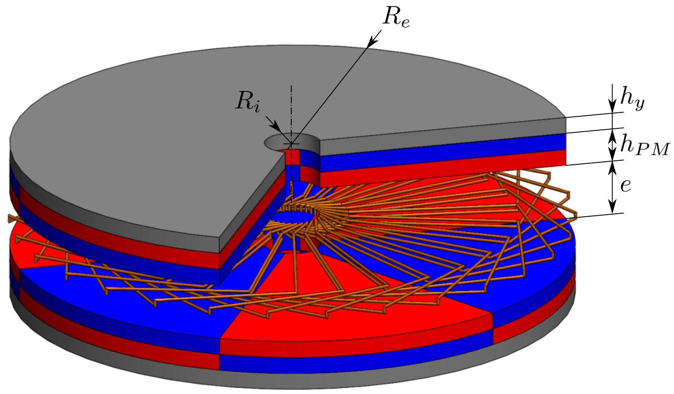

Fig. 5. Application: bearing with PMs arrangements attached to the stator and a single layer of phase windings.

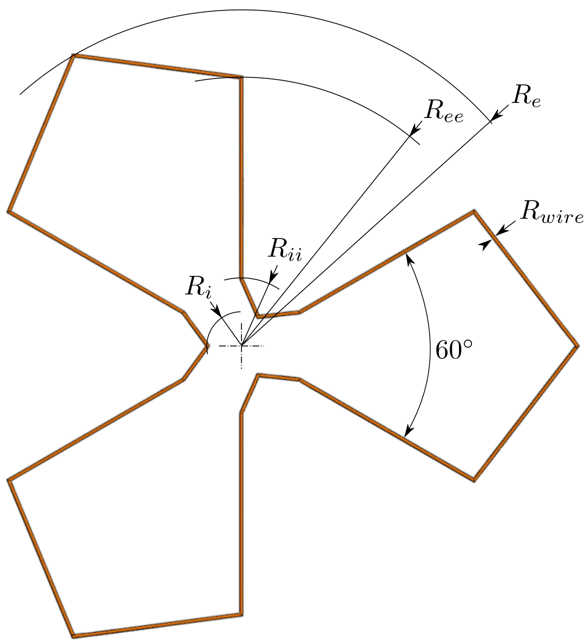

Fig. 6. Application: phase winding geometry.

A. Flux linkage validation

The general form of the flux linkage due to the PMs, based on a second order Taylor expansion of the magnetic field, is given in (23). As stated in section IV-B3, it only depends on z and α. Let us consider a single phase whose angular position maximizes the flux linked. The evolution of this flux for axial and radial displacements from -0.5 [mm] to 0.5 [mm] is obtained through finite element methods and shown in Fig. 7. The surface can be approximated in the least-squares sense by:

$$\Phi(\epsilon, z) = a + bz + c\epsilon, \tag{76}$$

where z as well as ϵ are expressed in meters and with:

$$a = 0.0000 \quad b = 0.1810 \quad c = 0.0000 \tag{77}$$

The norm of the residuals of this approximation related to the maximal flux yields 1.75%. The coefficient of the term in ϵ as well as the offset are null. Therefore, under small displacements assumption, the flux linkage reduces to:

$$\Phi(z) = bz = K_\Phi z, \tag{78}$$

which validates the model and allows determining the coefficient K_Φ.

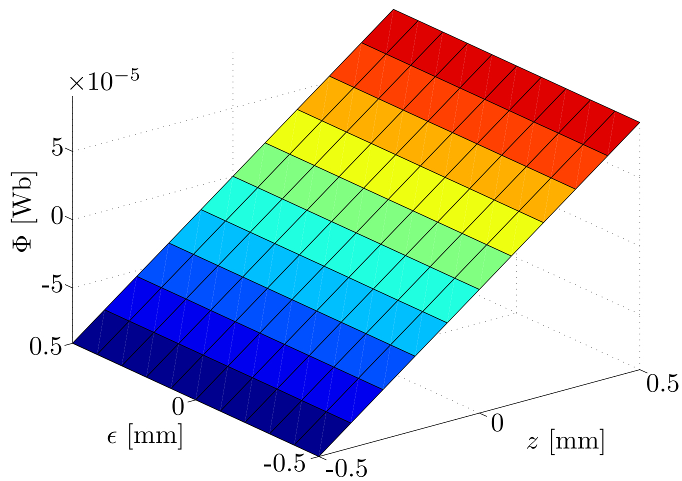

Fig. 7. Application: evolution of the flux Φ linked by a single phase with axial and radial displacements.

B. Parameters identification

Applying the methods described in section VII-C, the different parameters of the model are determined for the particular geometry being analyzed. The coefficient K_Φ was obtained previously through finite element methods. The winding phase resistance R is calculated using Pouillet's law and the cyclic inductance is determined with the energy-based method. The stiffness K_d is zero as there are no ferromagnetic parts at the armature. The results are listed in Table II. Besides, the rotor mass M is set arbitrarily to 1 [kg] as well as the damping factor C to 0 [Ns/m].

Table II
MODEL PARAMETERS.

R [mΩ]	L_c [μH]	K_Φ [Wb/m]	K_d [N/m]
32.4	0.659	0.181	0

C. Quasi-static analysis

In quasi-static conditions, the system (60) reduces to:

$$\begin{cases} F = -z \cdot \dfrac{N}{2} \cdot \dfrac{p^2 K_\Phi^2 \omega^2 L_c}{R^2 + (p\omega L_c)^2} \\ T = -z^2 \cdot \dfrac{N}{2} \cdot \dfrac{p^2 K_\Phi^2 \omega R}{R^2 + (p\omega L_c)^2} \end{cases} . \tag{79}$$

Therefore, the electrodynamic force F tends to bring the rotor back in its axial nominal position while the electrodynamic torque T contributes to decrease the spin speed and is then

This article has been accepted for publication in a future issue of this journal, but has not been fully edited. Content may change prior to final publication. Citation information: DOI 10.1109/TMAG.2016.2582727, IEEE Transactions on Magnetics

a braking torque. For a speed tending to infinity, the efforts become:

$$\begin{cases} F_\infty = -z \cdot \dfrac{N}{2} \cdot \dfrac{K_\Phi^2}{L_c} \\ T_\infty = 0 \end{cases} . \quad (80)$$

The maximal axial stiffness is thus given by $NK_\Phi^2/2L_c$ while the torque falls to zero. This is consistent with previous results [21]. Besides, taking the ratio of both expressions in (79) yields:

$$\frac{F}{T} = \frac{\omega L_c}{R} \cdot \frac{1}{z}. \quad (81)$$

Hence, an inductive behavior of the windings favors the restoring force while a resistive behavior favors the braking torque, degrading the performance of the EDB.

Let us apply the expressions of the quasi-static force and torque in (79) to the bearing being analyzed. Fig. 8 shows the evolution of the electrodynamic force (solid lines) and torque (dotted lines) with spin speed for several axial displacements. Purely inductive behavior appears for spin speeds greater than 500 000 [rad/s], yielding a maximal force of 248.5 [N] for an axial displacement $z = 1$ [mm]. For an identical z and a speed equal to 1000 [rad/s], which is a more reasonable speed, the force falls to 0.9 [N]. Nevertheless, it should be recalled that the aim of the thrust bearing studied in this paper is to provide a stabilizing effect and not to support the complete rotor. Therefore, the EDB can work properly even if the electrodynamic force is small.

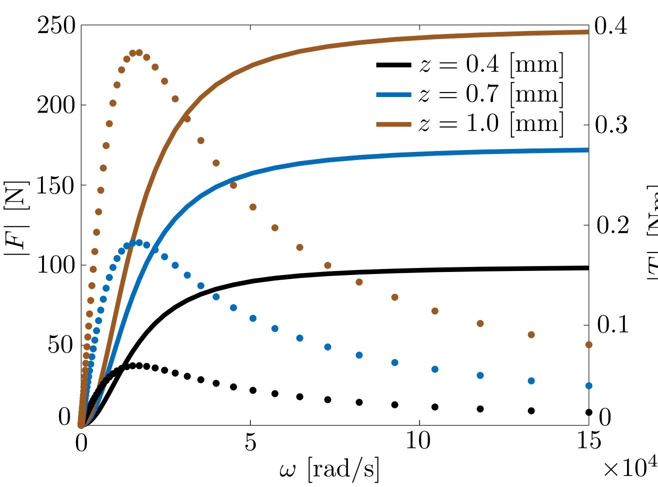

Fig. 8. Application: force (solid lines) and torque (dotted lines) evolution with spin speed in quasi-static conditions ($\dot{z} = 0$).

D. Root-locus analysis

Fig. 9 illustrates the root locus of the state-space model. It is derived by calculating the eigenvalues of the matrix $\mathbf{A}^{'}$ in (68) for different spin speeds $\omega \in [0, 10^6]$ [rad/s]. Among the four eigenvalues, two are always in the left half plane, far from the imaginary axis and are then stable. The other two are located near to this axis and are thus more relevant for the stability analysis. A zoom on the root locus for those roots is shown in Fig. 10. It can be observed that the thrust bearing is stable up to a spin speed equal to 16 395 [rad/s] at which the roots cross the imaginary axis. At higher speeds, the EDB becomes unstable and remains so for speed tending to infinity. This was already noticed in [21].

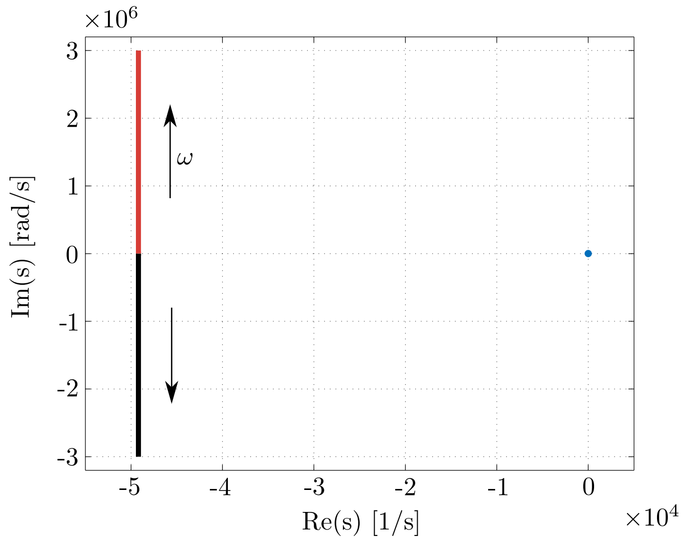

Fig. 9. Application: root loci of the EDB.

Unlike the radial electrodynamic bearings, the axial EDBs are stable at low speed, even with a damping factor equal to zero [13]. However, adding external damping allows improving dynamic stability. The effect on the relevant poles is illustrated in Fig. 10 for $C = 1$ [Ns/m]: the poles move to the left by an amount proportional to C, leading, in this case, to an unconditionally stable EDB. Therefore, the model presented in this paper allows determining, when it is required, the minimal damping factor ensuring stability for a targeted speed. Finally, this external damping between the stator and the rotor should preferably be contactless to be consistent with the magnetic bearing approach.

E. Copper losses estimation

The force and torque on the bearing rotor were given in Fig. 8 for different operating conditions. Let us now calculate the corresponding RMS current density on the wire cross section using the results from section VII-D. In quasi-static conditions, the RMS phase current I_{RMS} is obtained using (75) and (79):

$$I_{RMS} = \frac{1}{\sqrt{2}} \frac{zp\omega K_\Phi}{\sqrt{R^2 + (p\omega L_c)^2}}. \quad (82)$$

The resulting RMS current density J_{RMS} is given in Fig. 11. It is far above the value of $5[A/mm^2]$ that is usually considered as a maximum in the literature. As a result, the bearing would certainly not satisfy the thermal constraints, except at very low speeds or eccentricities. This confirms the assertion from subsection VIII-C, stating that this bearing should preferably be used as a stabilizer operating close to $z = 0$, combined with PM weight relievers e.g..

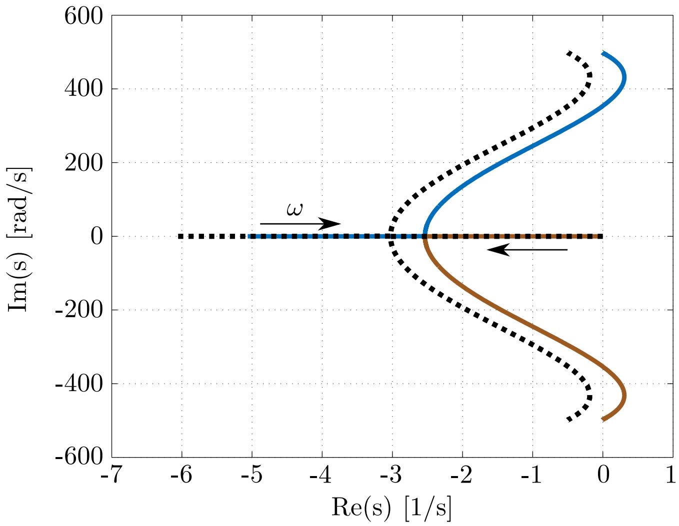

Fig. 10. Application: zoom on the interesting root loci of the EDB (solid lines), and effect of an external damping $C = 1$ [Ns/m] on the relevant poles (dotted lines).

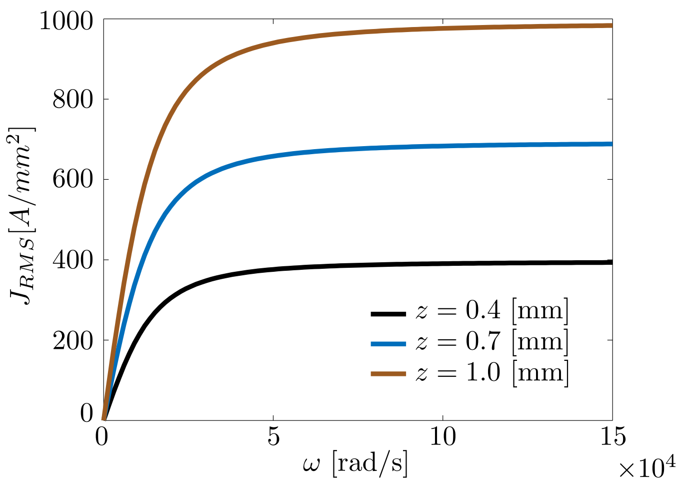

Fig. 11. Application: evolution of the RMS current density on the wire cross section in quasi-static conditions ($\dot{z} = 0$).

IX. Conclusion

This paper introduces a set of new null-flux electrodynamic thrust bearing topologies. Considering small axial and radial displacements, the general form of the PM flux linked by each winding phase is derived and validated through a practical case study. Based on the PM flux linkage, a state-space representation describing the axial dynamics of a thrust bearing is derived. Compared to existing models, it requires no assumptions on the rotor axial kinematics and can be applied to study a wider range of bearings, including those with an arbitrary number of phases and ferromagnetic yokes. As a result, electrodynamic thrust bearings with potentially increased performance are now within the scope of a linear model. Besides, being linear, it allows straightforward stability analysis.

The model depends on eight parameters whose identification is detailed in the paper. This reduced set of parameters fully describes the dynamics as well as the quasi-static behavior and therefore enables analyzing the performance of the EDB, including their stiffness and stability properties. Various bearings can thus be objectively compared and it becomes easier to determine the most suitable solution for an application. In particular, this model could be exploited in a process of optimal design of an electrodynamic thrust bearing.

Finally, future research prospects include studying the impact of the tilt angle on the bearing operation and validating the model through experimental results.

Appendix
Derivation of the Transformed Flux Vector

The transformed magnetic flux vector is obtained through (23) and (34):

$$\mathbf{\Phi^s} = \mathbf{U^{-1}\Phi}. \tag{83}$$

Knowing the identity:

$$\cos(x) = \frac{e^{jx} + e^{-jx}}{2}, \tag{84}$$

the vector $\mathbf{\Phi}$ can be expressed as:

$$\mathbf{\Phi} = zK_\phi(\mathbf{G} + \mathbf{D}), \tag{85}$$

where the components of $\mathbf{G}$ and $\mathbf{D}$ are:

$$\begin{aligned} G_k &= \frac{e^{j\left(\frac{2\pi}{N}(k-1)+p(\delta_0-\alpha)\right)}}{2}; \\ D_k &= \frac{e^{-j\left(\frac{2\pi}{N}(k-1)+p(\delta_0-\alpha)\right)}}{2}, \end{aligned} \tag{86}$$

with $k = \{1, \ldots, N\}$. Let us calculate the components of $\mathbf{U^{-1}G}$ and $\mathbf{U^{-1}D}$ separately:

$$\begin{aligned} \left[\mathbf{U}^{-1}\mathbf{G}\right]_k &= \sum_{i=1}^{N} U_{ki}^{-1} G_i \\ &= \frac{e^{-jp(\alpha-\delta_0)}}{2\sqrt{N}} \sum_{i=1}^{N} e^{j\frac{2\pi}{N}(i-1)(k-1)} e^{j\frac{2\pi}{N}(i-1)} \\ &= \frac{e^{-jp(\alpha-\delta_0)}}{2\sqrt{N}} \sum_{i=1}^{N} e^{j\frac{2\pi}{N}(i-1)k} \\ &= \frac{\sqrt{N}}{2} e^{-jp(\alpha-\delta_0)}, \qquad \text{if } k = N \end{aligned} \tag{87}$$

and 0 otherwise. The term $\mathbf{U}^{-1}\mathbf{D}$ is derived in a similar way:

$$\begin{aligned} \left[\mathbf{U}^{-1}\mathbf{D}\right]_k &= \sum_{i=1}^{N} U_{ki}^{-1} D_i \\ &= \frac{e^{jp(\alpha-\delta_0)}}{2\sqrt{N}} \sum_{i=1}^{N} e^{j\frac{2\pi}{N}(i-1)(k-1)} e^{-j\frac{2\pi}{N}(i-1)} \\ &= \frac{e^{jp(\alpha-\delta_0)}}{2\sqrt{N}} \sum_{i=1}^{N} e^{j\frac{2\pi}{N}(i-1)(k-2)} \\ &= \frac{\sqrt{N}}{2} e^{jp(\alpha-\delta_0)}, \qquad \text{if } k = 2 \end{aligned} \tag{88}$$

This article has been accepted for publication in a future issue of this journal, but has not been fully edited. Content may change prior to final publication. Citation information: DOI 10.1109/TMAG.2016.2582727, IEEE Transactions on Magnetics

and 0 otherwise. Substituting (87) and (88) into (83) yields:

$$\mathbf{\Phi^s} = z\frac{K_\Phi\sqrt{N}}{2}\begin{bmatrix} 0 \\ \exp(jp(\alpha-\delta_0)) \\ 0 \\ \vdots \\ 0 \\ \exp(-jp(\alpha-\delta_0)) \end{bmatrix}. \qquad (89)$$

REFERENCES

[1] G. Schweitzer and E. H. Maslen, *Magnetic bearings: theory, design, and application to rotating machinery*. New York, NY, USA: Springer-Verlag, 2009.

[2] R. Moser, J. Sandtner, and H. Bleuler, "Optimization of repulsive passive magnetic bearings," *IEEE Trans. Magn.*, vol.42, no.8, pp.2038-2042, Aug. 2006.

[3] J.-P. Yonnet, "Passive magnetic bearings with permanent magnets," *IEEE Trans. Magn.*, vol.14, no.5, pp.803-805, Sep. 1978.

[4] K. D. Bachovchin, J. F. Hoburg, and R. F. Post, "Magnetic fields and forces in permanent magnet levitated bearings," *IEEE Trans. Magn.*, vol.48, no.7, pp.2112-2120, Jul. 2012.

[5] S. Earnshaw, "On the nature of the molecular forces which regulate the constitution of the luminiferous ether," *Trans. Camb. Phil. Soc.*, vol.7, pp.97-112, 1842.

[6] R. F. Post and D. D. Ryutov, "Ambient-temperature passive magnetic bearings: theory and design equations," *Proc. 6th Int. Symp. Magn. Bearings*, Cambridge, Massachusetts, USA, Aug. 5-7, 1998.

[7] T. A. Lembke, *Design and analysis of a novel low loss homopolar electrodynamic bearing*, Ph.D. dissertation, Royal Inst. Tech., Sweden, 2005.

[8] C. Murakami and I. Satoh, "Experiments of a very simple radial-passive magnetic bearing based on eddy currents," *Proc. 7th Int. Symp. Magn. Bearings*, ETH, Zurich, Switzerland, Aug. 23-25, 2000.

[9] A. Filatov, *Null-E Magnetic Bearings*, Ph.D. dissertation, University of Virginia, Blacksburg, VA, 2002.

[10] V. Kluyskens and B. Dehez, "Dynamical electromechanical model for magnetic bearings subject to eddy currents," *IEEE Trans. Magn.*, vol. 49(4), pp. 1444-1452, 2013.

[11] N. Amati, X. D. Lepine, and A. Tonoli, "Modeling of electrodynamic bearings," *J. Vib. Acoust.*, vol. 130(6), 2008.

[12] J. G. Detoni, F. Impinna, A. Tonoli, and N. Amati, "Unified modelling of passive homopolar and heteropolar electrodynamic bearings," *J. Sound and Vibrations*, vol. 331(19), pp. 4219-4232, 2012.

[13] C. Dumont, V. Kluyskens, and B. Dehez, "Linear state-space representation of heteropolar electrodynamic bearings with radial magnetic field," *IEEE Trans. Magn.*, vol. 52, no. 1, 2016.

[14] J. G. Detoni, "Progress on electrodynamic passive magnetic bearings for rotor levitation," *Proc. Inst. Mech. Eng., Part C: J. Mech Eng. Sci.*, vol. 228, pp. 1829-1844, 2014.

[15] G. Sacerdoti, A. Catitti, and L. L. Soglia, "Self-centering rotary magnetic suspension device," Italian patent 49943/71, Apr. 24, 1971.

[16] K. R. Davey, "Designing with null-flux coils," *IEEE Trans. Magn.*, vol.33, no.5, pp.4327-4334, 1977.

[17] R. F. Post, "Passive magnetic bearings for vehicular applications," *LLNL Technical Report UCRL-ID-123451*, 1996.

[18] H. K. Asper, "Passive dynamically stabilizing magnetic bearing and drive unit," World patent 2003/098064, Nov. 27, 2003.

[19] J. Sandtner and H. Bleuler, "Electrodynamic passive magnetic bearing with planar halbach arrays," *Proc. 9th Int. Symp. Magn. Bearings*, Lexington, Kentucky, USA, Aug. 2004.

[20] K. D. Bachovchin, J. F. Hoburg, and R. F. Post, "Stable levitation of a passive magnetic bearing," *IEEE Trans. Magn.*, vol.49, no.1, pp.609-617, Jan. 2013.

[21] F. Impinna, J. D. Detoni, N. Amati, and A. Tonoli, "Passive magnetic levitation of rotors on axial electrodynamic bearings," *IEEE Trans. Magn.*, vol.49, no.1, pp.599-608, Jan. 2013.

[22] D. C. White and H. H. Woodson, *Electromechanical energy conversion*. Wiley, New York, 1959.

Joachim Van Verdeghem was born in Belgium in 1993. He is currently working on the development of an axial electrodynamic suspension in collaboration with the Center for Research in Mechatronics (CEREM) at the Ecole Polytechnique de Louvain (EPL), Louvain-la-Neuve, Belgium.

Corentin Dumont was born in Belgium in 1989. He received the electromechanical engineering degree in 2012 from the Université catholique de Louvain (UCL), Louvain-la-Neuve, Belgium, and is a Ph.D. student at the Center for Research in Mechatronics (CEREM) at the Ecole Polytechnique de Louvain (EPL). His research focuses on magnetic bearings.

Virginie Kluyskens was born in Belgium, in 1980. She received the electromechanical engineering degree in 2004 and the Ph.D. degree in 2011 from the Université catholique de Louvain (UCL), Louvain-la-Neuve, Belgium.
She is currently Senior Researcher at the Center for Research in Mechatronics (CEREM) at the Ecole Polytechnique de Louvain (EPL). Her research interests are in the field of passive magnetic bearings.

Bruno Dehez was born in Belgium, in 1975. He received the degree in electromechanical engineering and the Ph.D. degree from the Université catholique de Louvain (UCL), Louvain-la-Neuve, Belgium, in 1998 and in 2004, respectively.
He is currently a Professor at the Center for Research in Mechatronics (CEREM) at the Ecole Polytechnique de Louvain (EPL). His research interests are in the field of design and optimization of electromagnetic devices, and particularly of electrical machines and actuators.